



# Specific Fuel Oil Consumption Models for Simulating Energy Consumption of Wellboats

L. Æsøy   H. Zhang   A.R. Nerheim

*Department of Ocean Operations and Civil Engineering, Norwegian University of Science and Technology, N-6025 Ålesund, Norway. E-mail: {lene.asoey, hozh, ann.r.nerheim}@ntnu.no*

---

## Abstract

Aquaculture is the second-largest export industry in Norway. The Norwegian Government has committed to reducing CO<sub>2</sub> emissions by 55% by 2030 through the Paris Agreement. Wellboats are highly specialised vessels transporting and handling live fish, and one of the main contributors to CO<sub>2</sub> emissions within the fish farming production. For the aquaculture industry to be able to maintain or increase food production within future emission limits, the implementation of novel fuel concepts and the enhancement of energy efficiency measures are essential.

This study focuses on the validation of Specific Fuel Oil Consumption (SFOC) models used in simulations for assessing fuel reduction potentials. The novelty of this study was the development of SFOC models using data collected from two different engines. Further, the SFOC models were validated using data collected from a wellboat. The aim was to obtain a validated model that can be used to evaluate the fuel reduction potential of alternative engine configurations in existing vessels.

Two SFOC models were developed and tested against operational vessel data in simulations. The simulation results were compared and validated against measured onboard fuel consumption data. Findings showed that the SFOC models gave satisfactory results in fuel consumption prediction. Thus, the model can predict fuel consumption for various engine sizes and configurations onboard the vessel. If included in a power management system, the SFOC models could give real-time recommendations for fuel consumption reduction for wellboats.

*Keywords:* Energy efficiency, aquaculture, fuel reduction, renewable energy, maritime fuel, live fish carrier.

---

## 1 Introduction

Utilising ocean space to increase sustainable food production presents challenges in meeting the emission reduction targets described in the Paris Agreement (UN, 2015). The goal set by the International Maritime Organization (IMO) is to reduce the annual Green House Gas (GHG) emissions of international shipping by 50% by 2050 (IMO, 2018). To meet the Paris Agreement, the Norwegian Government has committed to reducing the CO<sub>2</sub> emissions by 55% by 2030 as compared to 1990 levels (Regjeringen, 2021, 2022; Miljødirektoratet, 2023; UN, 2015). To achieve the emission reduction

goals, the around 1100 vessels operating in Norway today must be converted to 700 low- and 400 zero-emission vessels (Cluster, 2022; NHO, 2022).

The Norwegian government aims to quintuple fish production by 2050 (Industri, 2016). Reports show an annual average growth rate of 3.5% of the global aquaculture between 2016-2021 and a foretasted increase in salmon production between 2019-21 to 2031 by 2.7%, (Mair et al., 2023). Additionally, DNV (2021) forecasts a global marine aquaculture production growth from 29 Mt in 2020 to 74 Mt in 2050. The anticipated increase in aquaculture production will result in increased maritime traffic, which poses emissions challenges unless

vessels adopt low or zero-emission fuels.

Norway's more than 90 wellboats contribute significantly to CO<sub>2</sub> emissions (Winther et al., 2020). The emissions increased by 67% from 2017 to 2021. Given their 20-30-year lifespan, emission-cutting actions are crucial (StakeholdersAS and ZeroKyst, 2022). Despite a shift to diesel-electric propulsion and "battery-ready" systems in new wellboats (Sølvtrans, 2023), the overall use of fossil fuels is rising. Investigating and implementing CO<sub>2</sub> reduction measures is essential to meet industry emission targets. Such evaluation for the emission reduction potential of an existing wellboat requires knowledge about energy consumption, operational profiles and specific fuel oil consumption (SFOC) of the engines.

Mylonopoulos et al. (2023) provides a comprehensive literature review of modelling and optimisation methods of power and propulsion systems of ships, concluding that ship powertrains are becoming increasingly complex, suggesting the need for more data-driven approaches in future research directions. In their review of ship fuel consumption models, Fan et al. (2022) propose future research directions, suggesting the integration of specific fuel consumption (SFC) models with energy efficiency optimisation methods. Both Kim and Roh (2020) and Lu et al. (2015) present ISO standards for estimating the Fuel Oil Consumption (SFC) of a Ship (ISO, 2015). However, these methods are based on estimating the speed and power of a ship using sea trial data. Hence, the models are based on ship resistance calculations, not SFOC measurements from the power generators. Ghimire et al. (2022) is employing a quadratic polynomial equation utilising the SFOC datasheet values provided by Wärtsilä. However, the dataset only covers loads down to 50%. Engine manufacturers usually provide SFOC data for engine loads above 50% load, and only in a few cases down to 25% (Æsøy et al., 2022; Nogva, n.d.; Dedes et al., 2012). Doundoulakis and Papaefthimiou (2022) presents SFOC models using regression analysis of engine data provided by the three engine manufacturers, Wärtsilä, Caterpillar and MAN. These models use datasheet values from engine manufacturers which only provide values for engine loads of 50% and above. However, these SFOC models have only been extended to provide calculated SFOC values down to 20%. The data collection and analysis performed by Æsøy et al. (2023) of a wellboat in operation showed that engines also were operated on loads lower than 25% and that the fuel consumption at low loads gave a significant contribution to the total fuel consumption. Therefore, a model providing SFOC input for lower engine loads is essential for predicting fuel consumption.

Law (2022) has described a methodology on how to

develop valid and credible simulation models following a 7-step approach. Æsøy et al. (2022) presented a simulation framework for evaluating the fuel and emission reduction potentials of a wellboat using a simple SFOC model based on laboratory experiments on a small engine, ref. (Nogva, n.d.). The simulation framework uses Simulink for a ship energy system simulation, employing a graphical modelling approach with default Runge-Kutta integration. It represents a network of power generators and consumers controlled by a power system and focuses on energy consumption and an optimised load-balancing solution.

The present study is motivated by the existing gaps in SFOC modelling, especially on lower loads, and contributes to the development of more effective tools for optimising ship energy efficiency. The main focus is developing SFOC models for various engine sizes and validating the models using data obtained by Æsøy et al. (2023). Model validation compares the simulated fuel consumption to actual measurements. The previous simulation framework served as a tool to test and verify the new SFOC models (Æsøy et al., 2022).

The overall goal is to simulate the accumulated fuel consumption using the SFOC models as input in the simulation framework and to compare the results with actual fuel consumption measurements from the same period. The SFOC models will further be used to evaluate the potential of increased energy efficiency of different engine configurations. Alternative engine configurations will be analysed using the same operational profile and input data for comparison. The results can be used to optimise the Power Management System (PMS).

The main objective of this study is to develop and evaluate two SFOC models through the simulation framework presented by Æsøy et al. (2022) using the collected data presented in Æsøy et al. (2023). One SFOC model is based on the SFOC model by Æsøy et al. (2022) but has now been adjusted to fit the simulated engine sizes. A second SFOC model is developed from logged SFOC data from another vessel with a similar sized and type of engine as the data collected from the wellboat used in Æsøy et al. (2023).

## 2 Materials and Methods

The following research approach and steps have been followed in the previous and present work, as illustrated in Figure 1:

- 1: A fuel consumption simulation framework was proposed and tested, implementing a model of the vessel energy system (Æsøy et al., 2022).
- 2: Real vessel data collection from a wellboat in operation was conducted in a field study and en-

ergy profiles were identified through data analysis (Æsøy et al., 2023).

- 3: The simulation framework was revised to represent the vessels’ specific energy system configuration and fuel consumption prediction simulations were conducted (present study).
- 4: Two SFOC models were developed to supply models for engines with an unknown fuel consumption profile. The models were based on lab measurements and engine data collected from another vessel (objective in the present study).
- 5: The simulated fuel consumption was compared with measured fuel consumption data to evaluate the SFOC models (objective of the present study).

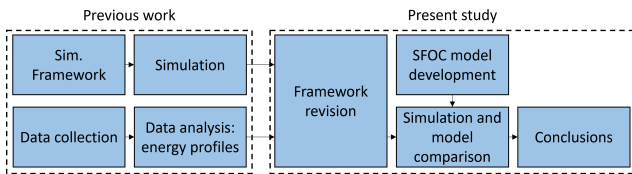


Figure 1: Overview of previous and present work.

In the present study, the following approaches for SFOC model development have been followed:

- 1: Make measurements in the lab and collect fuel consumption data from a ship in service.
- 2: Propose an SFOC model equation.
- 3: Fit the SFOC model to measurements.
- 4: Validate the SFOC model using total fuel consumption data from the vessel over a given period.

As a basis for the previous work, a field study was conducted to collect the needed energy consumption data (Æsøy et al., 2023). The collected data include total consumer load, power generators running signal, GPS data from the AIS system and fuel consumption measurements. Figure 2 shows the vessel layout of the wellboat under study (Vessel A) and its primary power consumer, power generation system and fuel measurement setup. Vessel A has a diesel-electric power system powered by four main diesel generators (MG) and one port/emergency generator (EG), all distributed through the main switchboard (SB). The four main generators and the emergency generator on Vessel A are further labelled  $N_{A1}$ - $N_{A4}$  and  $N_{AEG}$ , respectively. Vessel A were not equipped with sensors to measure or log the continuous fuel consumption from the engines installed onboard, which could be used to derive SFOC models. Therefore, two SFOC models using different modelling approaches from different-sized engines were developed, validated and compared with accumulated measurements from Vessel A in this study. The consumer load, engine running signal and the developed

SFOC models serve as inputs for the simulation framework.

To find the SFOC model equations and fit them to the measured data, a systematic approach was employed. The process included:

- 1: SFOC model development based on datasheets from engine manufacturers, and the measured fuel consumption data from other engines.
- 2: SFOC modelling adaptation to fit Vessel A’s engine size.
- 3: Simulation framework adjustments to fit Vessel A’s engine setup (number of engines, sizes, power distribution function).
- 4: Total fuel consumption simulations using the simulation framework.
- 5: Validation of the SFOC models against the measured accumulated fuel consumption data on Vessel A.

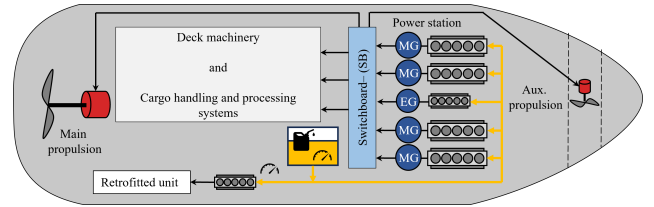


Figure 2: Simplified vessel layout of the power generation system and the primary power consumers for Vessel A. The power is generated by four main diesel generators (MG) and one emergency diesel generator (EG) and distributed through the main switchboard (SB). Updated vessel layout based on Figure 1 in Æsøy et al. (2023) now including the EG, a retrofitted unit and fuel measurement setup.

In another modelling approach, digitally logged fuel consumption and power data from another vessel (Vessel B) were used. This dataset contains digitally logged data for three weeks with a 1 Hz frequency of one of the installed power generators onboard Vessel B. The data includes measured fuel consumption (FC) and engine load ( $P_G$ ), as shown in Figure 3. A digital log recorded the fuel consumption measured by a Coriolis fuel flow meter (Henry et al., 2000). The power was measured and logged through the main switchboard (SB), thus including the generator efficiency ( $\eta_{GB}$ ). Data sheets from the engine manufacturer ( $N_B$ ) provide SFOC data of the produced engine power ( $P_E$ ). Hence, before comparing the logged data with the datasheets, the datasheet value needs to be adjusted to include the generator efficiency ( $\eta_{GB}$ ).

Power and fuel consumption measurements were conducted on a 71 kW John Deer engine ( $N_C$ ) in the

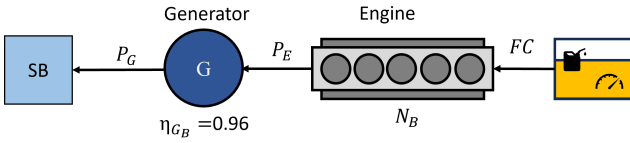


Figure 3: The power generator setup on Vessel B includes the engine  $N_B$ , which utilises fuel consumption (FC) to generate power  $P_E$ . Subsequently, this power is then transformed into electric power  $P_G$  by the generator with an efficiency  $\eta_{G_B}$  and supplied to the main switchboard (SB).

hybrid power laboratory at NTNU Aalesund. The power generator setup for engine  $N_C$  is the same as shown for  $N_B$  (refer to Figure 3). However, the fuel measurement setup is different. The fuel consumption of engine  $N_B$  was measured by a Coriolis fuel flow meter, while engine  $N_C$  ran under steady-state conditions for 30 minutes for each measured power load (recorded at the switchboard). The fuel level in the tank was measured at the start and stop times to determine fuel consumption over the period.

The data collected from Vessel A during the field study included power and fuel consumption data. Additionally, datasheets from the manufacturer of all the installed generators in Vessels A and B, and in the hybrid lab were obtained. An overview of the collected data can be found in Table 1.

The data collected from all the engines ( $N_{A_1}$ - $N_{A_4}$ ,  $N_{A_{EG}}$ ,  $N_B$  and  $N_C$ ) were measured through the main switchboards on Vessel A, Vessel B and in the hybrid laboratory, ref. Figures 2 and 3. Hence, the measured engine load is the power produced by the generators ( $P_G$ ) and delivered to the main switchboard (SB). Thus, the generator efficiencies ( $\eta_G$ ) are accounted for in the collected data. The datasheets on the main engines ( $N_{A_1}$ - $N_{A_4}$ ) gave engine-specific power generator testing data, provided by the manufacturer at delivery to the shipbuilder, and thus included the generator efficiency. However, the datasheet for engines  $N_{A_{EG}}$ ,

$N_B$  and  $N_C$  gave SFOC values per produced engine power unit ( $P_E$ ). Therefore, in this study, the generator efficiencies were used to calculate the SFOC values in g/kWh, where the kWh represents power delivered to the switchboard ( $P_G$ ). Hence, the SFOC values and measurements given in this paper include the generator efficiency.

The first model,  $SFOC_1$ , was derived based on measurements conducted on engine  $N_C$  in the hybrid power laboratory at NTNU Aalesund. The second model,  $SFOC_2$ , was developed based on fuel consumption data from another vessel (Vessel B). Table 2 and Table 3 show an overview of which engine data the two models were based on. The motivation for this approach was to create a combined SFOC model that could be used to analyse fuel consumption in maritime vessels where onboard detailed logging systems have not been installed (yet), such as Vessel A. The objective was to develop more accurate SFOC models, especially on the low loads, and models that could be adapted to several engine sizes. These models are input data for the framework tool for simulating fuel consumption and providing insight into overall fuel consumption and emissions reduction potential.

The SFOC curve obtained from the experiments on engine  $N_C$  was further adapted to fit the onboard engines ( $N_{A_1}$ - $N_{A_4}$ ,  $N_{A_{EG}}$ ) using the SFOC data from the engine manufacturer. This SFOC model ( $SFOC_1$ ) was fitted to the manufacturer's data of the onboard engines of Vessel A using vertical translation as shown in Equation (1). Here,  $H(P)$  represents the SFOC-curve obtained by [Æsøy et al. \(2022\)](#), and  $\Delta C_1(75)$  represents the difference between the SFOC values of the previous and present model at engine power load  $P = 75\%$  shown in Equation (2).

$$SFOC_1(P) = H(P) + \Delta C_1(75) \quad (1)$$

$$\Delta C_1(75) = C_{N_A}(75) - C_{N_C}(75) \quad (2)$$

The second SFOC model ( $SFOC_2$ ) used regression analysis on data logged onboard a different vessel (Vessel B) of a similar-sized engine ( $N_B$ ) from another en-

Table 1: Data collection overview showing the data source, e.g., from which engines and vessels, and their application for creating and adapting the SFOC models.

Location	Power source	Activity	Application
Vessel A (Wellboat under study)	Main Engines ( $N_A$ ), and Emergency Generator ( $N_{A_{EG}}$ )	Data collection (Vessel A)	Adjust SFOC models and run simulations
		Datasheets collected ( $N_A$ and $N_{A_{EG}}$ )	
Vessel B	Engine ( $N_B$ )	Data collection (Vessel B)	Develop models $SFOC_1$ and $SFOC_2$
		Datasheet collected ( $N_B$ )	
Hybrid Power LAB	Engine ( $N_C$ )	Conducted experiments	
		Datasheet collected ( $N_C$ )	

Table 2: SFOC model overview showing which engine data the models are based on.

SFOC Model	Model elements	Collected Engine Data	Datasheet values
SFOC <sub>1</sub>	$g(P)$	Engine $N_C$ (Hybrid Lab)	Engine $N_C$ (Hybrid Lab)
	$\Delta C_1(75)$		Engine $N_C$ (Hybrid Lab), Engine $N_A$ and $N_{AEG}$ (Vessel A)
SFOC <sub>2</sub>	$R(P)$	Engine $N_B$ (Vessel B)	Engine $N_B$ (Vessel B)
	$\Delta C_2(85)$		Engine $N_B$ (Vessel B), Engine $N_A$ and $N_{AEG}$ (Vessel A)

Table 3: SFOC model overview showing which engine data the models are based on, and which data were used to run the simulations.

Data description	SFOC <sub>1</sub> Model	SFOC <sub>2</sub> Model	Run simulations
Vessel A: Operational power consumption data, total fuel consumption data and manual log of operations.			x
Vessel A: Datasheet from the main engines $N_{A1} - N_{A4}$ .	x	x	
Vessel A: Datasheet from the emergency engine $N_{AEG}$ .	x	x	
Vessel B: Operational power and fuel consumption data from power generator $N_B$ .		x	
Vessel B: Datasheet from engine $N_B$ .		x	
Hybrid lab: Operational power and fuel consumption data from power generator $N_C$ .	x		
Hybrid lab: Datasheet from engine $N_C$ .	x		

engine manufacturer. The regression analysis used the curve fit function on the predefined function  $R(P)$  represented by Equation (3), where a, b, and c are coefficients, d is a constant, and P is a variable representing the engine power load. The curve-fit function used non-linear least squares analysis to fit the function to the data. To evaluate the regression analysis for each engine load, mean SFOC values ( $SFOC$ ) and standard deviation ( $\sigma$ ) per engine load were used.

$$R(P) = \frac{a}{b+P} + c \cdot P + d, \quad (3)$$

To adapt SFOC<sub>2</sub> to the engines installed onboard Vessel A,  $R(P)$  was shifted vertically using the data from the engine manufacturers. Vessel B only has one SFOC datasheet value ( $C_{N_B}$ ), which is at engine power load  $P = 85\%$ . This value was used to shift the curve vertically as described by Equations (4) and (5). The constant ( $d$ ) in Equation (3) changes with engine size.

Vessel A has SFOC datasheet values of  $C_{N_A}(75)$  and  $C_{N_A}(100)$  at engine power loads  $P = 75\%$  and  $P = 100\%$ , respectively. Linear interpolation with the data

was used to obtain an SFOC value  $C_{N_A}(85)$  at  $P = 85\%$ . The mentioned datasheet values can be found in Table 4.

$$SFOC_2(P) = R(P) + \Delta C_2(85) \quad (4)$$

$$\Delta C_2(85) = C_{N_A}(85) - C_{N_B}(85) \quad (5)$$

To adapt the original simulation framework to fit the engine configuration of Vessel A, the number and sizes of onboard engines were updated, as well as the type of SFOC model and the engine distribution function. The engine distribution function describes how the Power Management System (PMS) distributes the loads onto the engines. It uses the engine running signal input from the collected vessel data (Vessel A) and divides the load equally onto the engines, in the same way the PMS controls the load distribution onboard in real-time.

Validation of the SFOC models was performed by comparing the simulated accumulated fuel consumption using the various SFOC models with the mea-

Table 4: Specific Fuel Oil Consumption values from engine manufacturers where the generator efficiency has been accounted for.

Datasheet SFOC value $g/kWh$	
$C_{N_A}(75)$	196.8
$C_{N_A}(100)$	196.2
$C_{N_{AEG}}(75)$	236.1
$C_{N_{AEG}}(100)$	230.7
$C_{N_B}(85)$	192.7
$C_{N_C}(75)$	237.8
Interpolated SFOC values $g/kWh$	
$C_{N_A}(85)$	196.6
$C_{N_{AEG}}(85)$	233.9

sured total fuel consumption onboard Vessel A. The volumetric fuel consumption on Vessel A was measured onboard at given intervals using a flow meter. Manual logging procedures were employed to calculate the aggregated fuel consumption. The measurements of the accumulated fuel consumption were done manually every 24 hours by the crew. The accuracy of the exact time of reading the values could vary due to other urgent operations onboard.

The emergency generator of Vessel A shown in Figure 2 is significantly smaller than the main generators. Therefore, each SFOC model had to be adjusted to both the main generators and the emergency generators.

Table 1 provides an overview of all the collected data, which engine and vessel they were collected from, and their application in the various SFOC models. Table 2 and 3 show which engine data were used to create the various SFOC models. Simulations using the different SFOC models, SFOC<sub>1</sub> and SFOC<sub>2</sub>, are further referred to as Case 1 and Case 2, respectively.

### 3 Results and discussions

Fuel consumption data collected in a previous study (Æsøy et al., 2023), was used as input data in the present work. Total energy consumption data were automatically logged through the Power Management System (PMS), whereas accumulated fuel consumption was recorded manually in a log. Figure 4 shows the overall consumer load in the percentage of installed generator power. The grey area shows the field trip period covered in the manual log. The data was divided into three separate simulation periods, as shown in the figure. All these simulation periods are within the grey area in Figure 4, which corresponds to the field trip. The four lines marked with the letters (a)-(d) show the start and stop times of simulation periods used in the present analysis.

As shown in Figure 2 there is a retrofitted unit on board that operates independently of the PMS. This unit has its own power supply and fuel measurement. Thus, it was excluded from the present study. This retrofitted unit was sometimes in use while the accumulated fuel consumption was logged and measured. These periods have been excluded from the analysis.

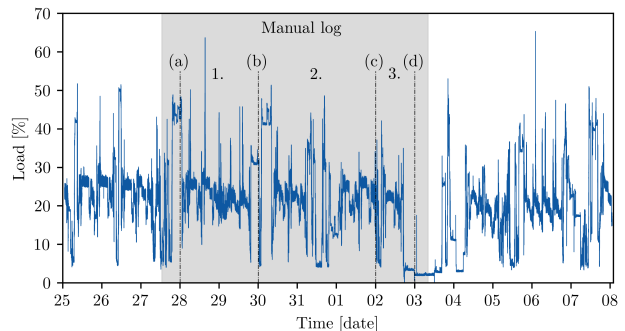


Figure 4: Total consumer load data for the entire dataset. The field trip period is highlighted in grey. The simulation periods are labelled 1-3, and the letters (a)-(d) denote start and stop times.

#### 3.1 SFOC-models

Figure 5 shows  $SFOC_1$  as a function of engine load. The green circles are the datasheet values of engine  $N_A$ , and the red diamonds represent the measured SFOC values from the lab experiment. The datasheet values of engine  $N_C$  are marked with an "x". Equation (1) describes how the model is adjusted to model the engine size installed onboard the wellboat (Vessel A). A fuel density of  $860 \text{ kg/m}^3$  was used to convert the SFOC data from  $g/kWh$  to  $m^3$  (BunkerOil, n.d.). The solid green line shows the  $SFOC_1$  model for Vessel A. The blue dash-dotted curve shows  $H(P)$  for the hybrid lab engine using vertical translation at engine load  $P = 75\%$ , as described in Equations (1) and (2). The values  $C_{N_A}(75) \text{ g/kWh}$  and  $C_{N_C}(75) \text{ g/kWh}$  are listed in Table 4.

Figure 6 shows fuel consumption data obtained from the engine ( $N_B$ ) from Vessel B. Engine  $N_B$  is of similar size and type of engine as the installed main engines on board the wellboat under study (Vessel A). Data density is visualised using hexagon bins and plotted with a logarithmic scale. Greater colour intensity corresponds to a higher quantity of data points. The darker blue visualises a trend, which indicates where the regression curve should fit. The arrows between 45% and 60% load in Figure 6 indicate what most probably are the effects of the engine shifting gear, which also is a source of variable SFOC measurements for each engine load.

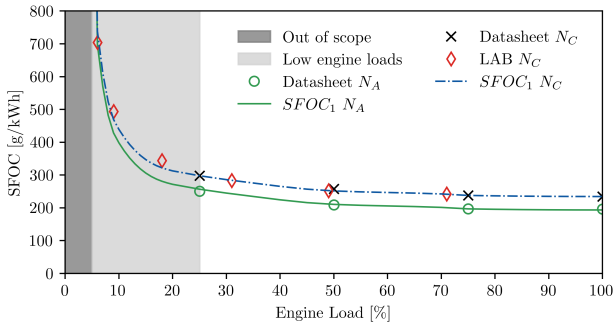


Figure 5: The SFOC model ( $SFOC_1$ ) based on measurements conducted on a 71 kW John Deer engine in the hybrid power lab at NTNU Aalesund, [Nogva \(n.d.\)](#); [Æsøy et al. \(2022\)](#).

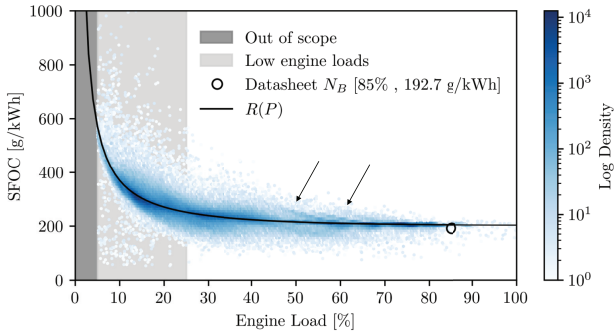


Figure 6: Specific Fuel Oil Consumption data from engine  $N_B$  on vessel B with a fuel consumption measurement system. The darker colour corresponds to a higher density of data points. The grey patches show the defined low engine loads (under 25%) and the loads out of scope (under 5%). The black curve represents the regression results ( $R(P)$ ) and data from engine manufacture (O).

Regression analysis of the predefined function presented in Equation (3) gave the following coefficients:  $a = 2017.69$ ,  $b = -0.00$ ,  $c = 0.18$  and  $d = 166.66$ . Figure 6 shows the Regression results ( $R(P)$ ) plotted with the data density points and the one data point available from the engine manufacturer (O).  $R(P)$  correlates with the darker trend. However, it does not pass through the centre of the manufacturer’s data point. Engine data from the manufacturer represent the most efficient and lowest value obtained when the engine was new. This may explain why the measured SFOC values in the present study deviate from the SFOC value given by the engine manufacturer.

The standard deviation for each engine load is calculated and shown with the regression model ( $R(P)$ ) in Figure 7 and thus assesses whether the regression

model is representative of the data. The red curve ( $SFOC$ ) shows the mean value of the Specific Fuel Oil Consumption data points for each engine load  $P$ . The blue areas represent the standard deviation ( $\sigma$ ) and the double standard deviation ( $2\sigma$ ) from the mean value. The blue curves show the relative standard deviation ( $\sigma/SFOC$ ) in percentage. Figure 7 shows that the regression curve is almost identical to the mean value of the measured data. Hence, the regression curve ( $R(P)$ ) represents a realistic model of the data for that specific engine. Thus, the regression model fits the data for that specific engine. However, the results show that the SFOC standard deviation in individual points is around 10% or less, except for a few cases at loads below 10%. The variation of the mean value and the deviation for engine loads greater than 85%, shown in Figure 7, are most probably due to a lack of data points, ref. Figure 6. Results show that for this engine, loads between 65 and 85% are preferable in terms of both specific fuel consumption and model accuracy.

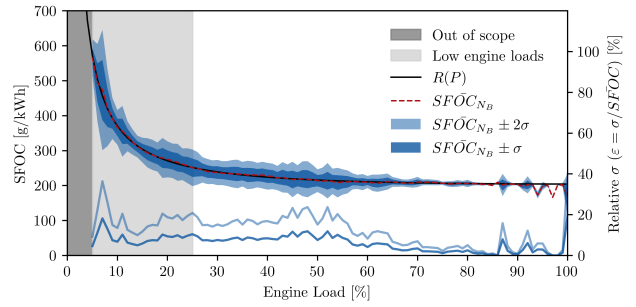


Figure 7: Standard deviation ( $\sigma$ ), double standard deviation ( $2\sigma$ ) and mean values ( $SFOC_{N_B}$ ) for each engine load ( $P$ ) plotted together with the regression results ( $R(P)$ ) for engine  $N_B$ .

Figure 8 shows the two SFOC models fitted to the engine data of the installed main engine onboard Vessel A. The green marks (O) are the data provided by the engine manufacturer ( $N_A$ ). The green curve is  $SFOC_1$  fitted to the engine data ( $N_A$ ), ref Equation (1). The dashed green curve representing  $SFOC_2$  is the regression result fitted to the engine data ( $N_A$ ) using Equation (4). The models presented in Figure 8 were input to the simulation framework, where  $SFOC_1$  and  $SFOC_2$  were used to simulate the total fuel consumption, Case 1 and 2, respectively.

Energy system parameters in the simulation framework presented by [Æsøy et al. \(2022\)](#) were set to represent the actual vessels’ engine setup. These parameters include the number of engines and the power capacity per engine. Data preparation and analysis revealed that the port/emergency generator ( $N_{AEG}$ ) powered the main switchboard during part of the field trip pe-

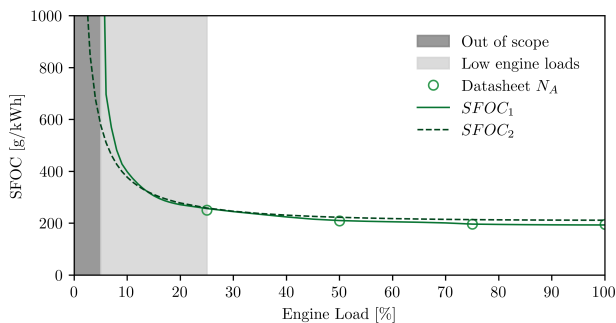


Figure 8: The Specific Fuel Oil Consumption (SFOC) models chosen for the simulation fitted to the main engine ( $N_A$ ) installed onboard Vessel A using the provided engine data (O) from the engine manufacturer. The green curve shows the  $SFOC_1$  model based on experimental measurements from the laboratory. The green dashed curve shows the  $SFOC_2$  model based on measured data from a similar engine ( $N_B$ ) from Vessel B, ref. Figure 6.

riod. Thus, the power distribution function was updated to include the main engine generators ( $N_A$ ) together with the emergency generator ( $N_{AEG}$ ).

### 3.2 Simulation results and model validation

The two SFOC models  $SFOC_1$  and  $SFOC_2$  were assessed individually by two separate simulations, Case 1 and Case 2, respectively. The simulation input remained the same for both cases, including the total consumer load and engine running signal. The outputs from the simulations were the accumulated fuel consumption, which was further compared to the measured total fuel consumption. Simulations were performed for separate operation periods, which together cover the total field trip period.

Figure 9 shows the simulation input for the simulation period for Case 1. The upper leftmost plot shows the total consumer load (presented as % of installed main generator capacity), followed by the engine running signal (1/0, on/off per engine) to the right. Below, the operational hours per engine load condition is presented as a histogram together with the  $SFOC_1$  and  $SFOC_2$  models for the main generators  $N_{A1}$ - $N_{A4}$  and the emergency generator  $N_{AEG}$ . The number of hours plotted in the histogram is per engine. Thus, the total amount of engine hours exceeds the duration of the field trip period, since more than one engine was running simultaneously. The grey area shows the defined low engine loads, where the engines run less efficiently

due to higher SFOC.

Figure 9 shows that the power generators ran 28.3 hours on loads below 25% during the six days of the field trip. Most of these hours accumulated while two engines were running, indicating an inefficient power supply due to need for engine redundancy for fish welfare and safety. There is also one period where one main generator is running below 25% while the vessel is at port. However, the load was too large to be provided by the installed port/emergency generator alone, and one of the main generators was therefore used to power the ongoing operations, e.g. hydraulic cranes. Hence, the vessel could benefit from a more powerful emergency generator for port operations, and a backup battery (for redundancy and peak-shaving). If a battery was installed the other operations could be supplied by one main engine instead of two to avoid engine loads below 25%, ref. the statistical analysis shown in Figure 7.

Figure 10 shows the simulation results for the total simulation period for Case 1 for each installed power generator. The leftmost column shows the engine load per installed engine, and the rightmost column shows the simulated Fuel Consumption results (FC) per engine, based on the specific fuel consumption model ( $SFOC_1$ ) for the simulation Case 1. Figure 10 shows how the  $SFOC_1$  values vary per engine load. The same plot can be shown for Case 2. However, due to the resolution, it will not show a significant difference from Figure 10. Hence, Cases 1 and 2 are better compared by plotting the accumulated fuel consumption, as shown in Figure 11, together with the measured fuel consumption onboard Vessel A.

The simulations presented in Figure 11 were based on the whole dataset, as given from (a) to (d) in Figure 4. Simulation results per simulation period and the total period for both Cases 1 and 2 are presented in Table 5. The results for the total simulation period show that the  $SFOC_1$  model underestimates the accumulated fuel consumption by 3.9% and the  $SFOC_2$  model by 0.9%, as compared to the measured fuel consumption on Vessel A. The  $SFOC_1$  model is based on measurements done in steady-state conditions in a laboratory on land, not taking transient values into account. Additionally, the model predicts SFOC values around the same as datasheet values from the engine manufacturer which represents more ideal conditions, ref. Figure 8. Hence, it is expected that the  $SFOC_1$  model will underestimate the accumulated fuel consumption under real conditions. As illustrated in Figure 8, the  $SFOC_2$  model predicts higher SFOC on higher loads and lower SFOC values on engine loads below 13% ( $P \leq 13\%$ ), which is expected when comparing the  $SFOC_2$  model to the datasheet value of engine  $N_B$ , ref Figure 6. The mea-



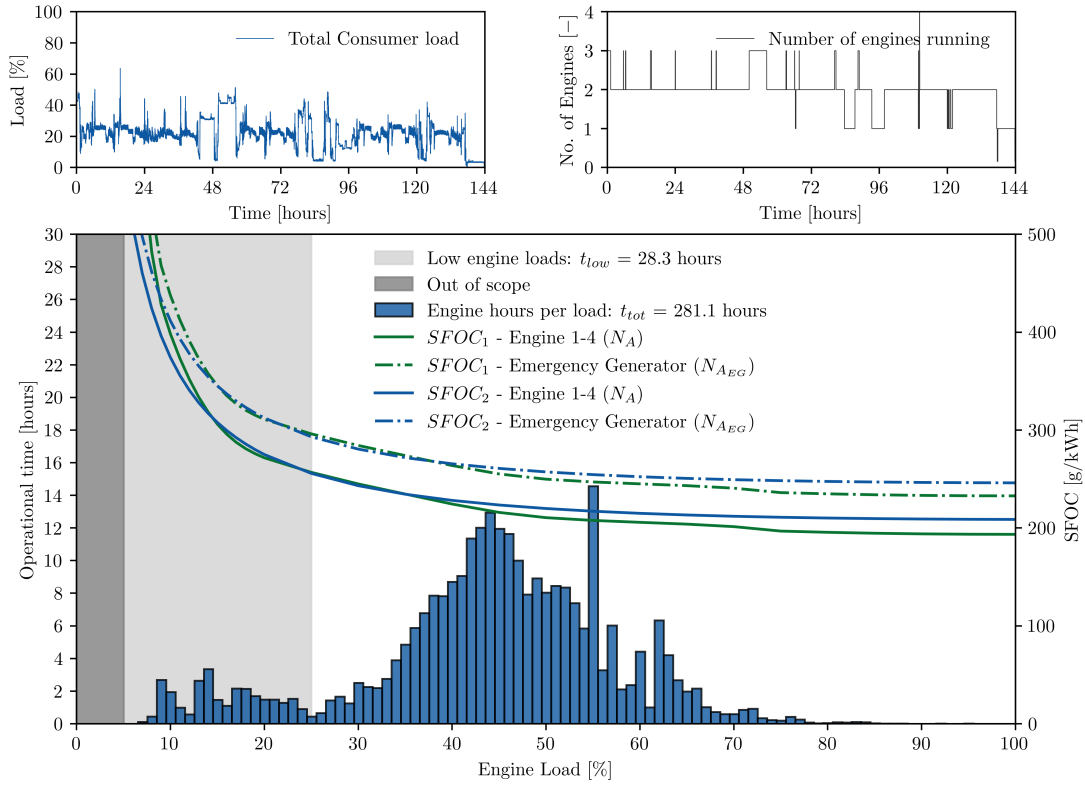


Figure 9: Simulation input for the total simulation period for Case 1 and Case 2.

Table 5: Simulation results compared to measured fuel consumption for the simulation periods. The deviations from actual measurements are given as percentages, where plus refers to over-simulated, and minus shows under-simulated results.

Simulation period	Accumulated Fuel Consumption [m <sup>3</sup> ]			
	Measured	Simulated Case 1	Simulated Case 2	Deviation differences Case 1 - Case 2
1 (48 h)	14.2	14.8 (+3.9%)	15.2 (+7.2%)	3.3%
2 (72 h)	23.1	21.1 (-8.6%)	21.8 (-5.6%)	3.0%
3 (24 h)	5.3	5.1 (-4.5%)	5.2 (-2.3%)	2.2%
Total (144 h)	42.6	40.9 (-3.9%)	42.2 (-0.9%)	3.0%

measured data on Vessel B shows that the  $SFOC_2$  model predicts greater than the given datasheet values from the engine manufacturer.

Table 5 shows the simulation results for each simulation period and the measured onboard fuel consumption. The deviation from measured fuel consumption for each simulation period can be explained by the manual logging of the measured fuel consumption. The exact time of the measurement can deviate due to the urgent tasks onboard the vessel. Hence, the total simulation, which is based on the longer time period, will give a more accurate comparison. This can especially be seen by comparing simulation periods 1 and 2 for Case 1 and by comparing Case 1 and 2 with each other

for each period. When Case 1 is over-simulating, Case 2 is also over-simulating for the same period, and vice versa. This shows that  $SFOC_2$  estimates a fuel consumption 2.2-3.3% higher than that of  $SFOC_1$ . Specifically, the deviation differences are 3.3%, 3.0%, 2.2%, and 3.0% for simulation periods 1, 2, 3, and the total period, respectively, ref Table 5.

Figure 12 shows the operational hours per engine load for (a) simulation period 1, (b) simulation period 2, (c) simulation period 3 and (d) the total simulation period. Figure 12(a) also shows the SFOC models for simulation Cases 1 and 2 for  $N_A$  and  $N_{A_{EG}}$ . The distribution of operational hours per engine load for each period is very different, especially on lower loads.

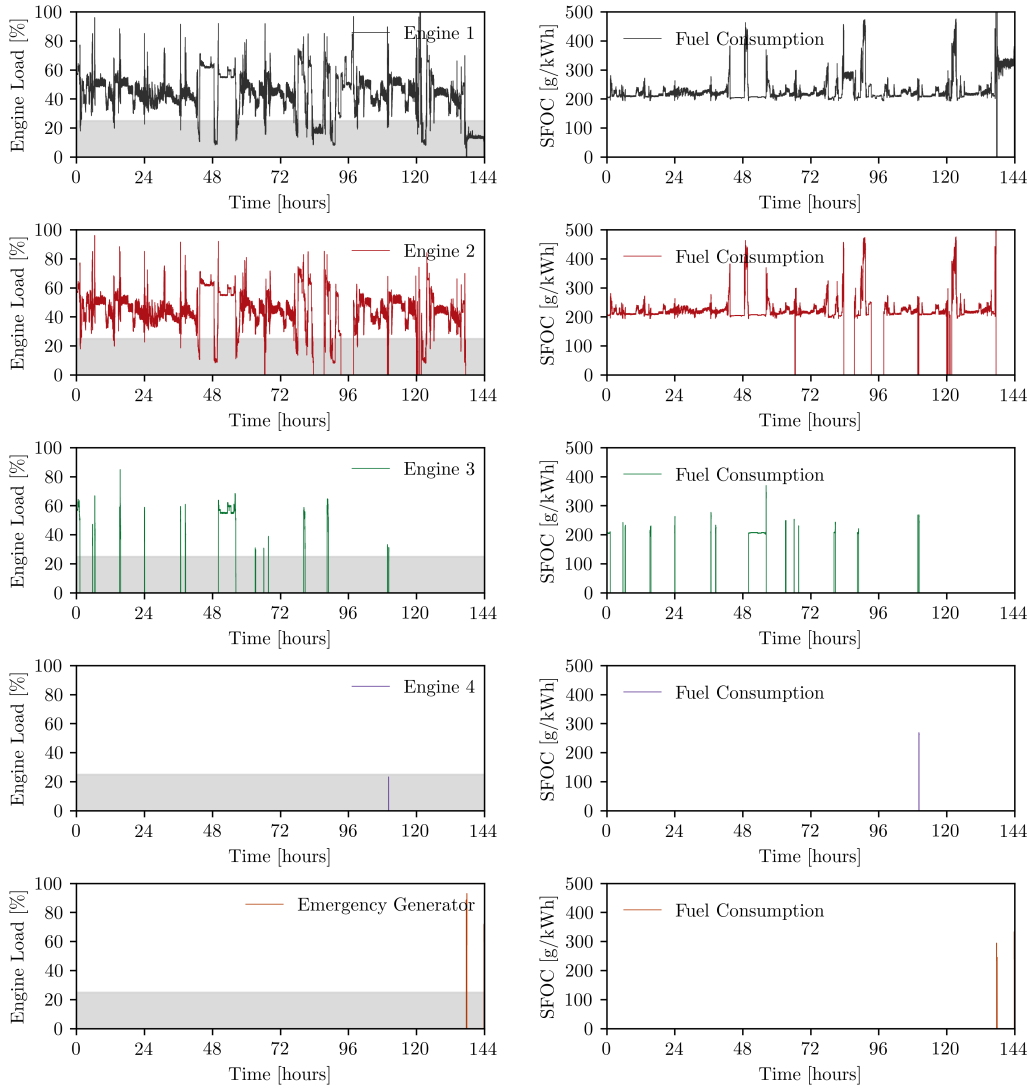


Figure 10: Simulation result for the total simulation period for Case 1.

This can explain the variation in the simulation results of 2.2-3.3% between the SFOC models. Simulation period 1 has only 1.8 hours on lower loads, and for most of the hours, the engine loads are between 32-65% where SFOC<sub>2</sub> have a higher SFOC estimation than SFOC<sub>1</sub>. As compared to simulation period 3 where more than 25% of the engine hours are run at lower loads where SFOC<sub>1</sub> have a higher SFOC estimation than SFOC<sub>2</sub>. It is also worth noticing that the model is less accurate on lower loads, ref. Figure 7.

The SFOC<sub>1</sub> model used for Case 1 is based on laboratory measurements and SFOC data from a significantly smaller engine ( $N_C$ ) than the main engines installed on Vessel A, and fitted to the installed engine size by SFOC data provided by the engine manufacturers ( $N_A$ ). This model assumption assumes that

the SFOC characteristics of the small laboratory engine and the installed engines onboard Vessel A are the same. Hence, this simplification may cause deviations between the simulated and the actual measured fuel consumption.

The SFOC<sub>2</sub> model used the actual fuel consumption data from a similar sized and type of engine ( $N_B$ ) on Vessel B. As shown in Figure 7, the results from the statistical analysis calculating the standard deviation for each engine load show a great variety of fuel consumption measurements within each engine load. The standard deviation is more than 10% for loads below 60%. The logged data show that most of the engines are operating below 65% load i.e. where the deviation is the highest, ref. histogram in Figure 10.

The dataset from the engine manufacturer ( $N_B$ ) only

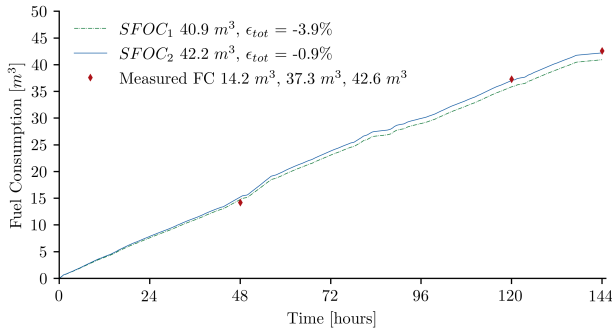


Figure 11: The simulated accumulated fuel consumption curves for Cases 1 and 2 for the total simulation period. The green dash-dotted curve represents Case 1, the SFOC<sub>1</sub> model, and the blue curve presents Case 2, the SFOC<sub>2</sub> model. The red dots show the recorded onboard fuel consumption data.

contained one data point. Equation (4) describes how the regression model was adjusted to model the installed engine sizes ( $N_A$  and  $N_{AEG}$ ) of Vessel A, using data from another engine  $N_B$ . This approach assumes that the one data point provided by the engine manufacturer of  $N_B$  was representative and comparable to similar types.

The installed emergency generator on Vessel A is more similar to the engine in the laboratory used to create the SFOC<sub>1</sub> model than the engine on Vessel B. For future simulations, this model may be better suited to simulate this type of engine. However, the running hours of the emergency generator compared to the main generators are negligible and would not affect the results of the total fuel consumption simulation significantly, ref. Figure 10. The SFOC<sub>2</sub> model is based on a similar size and type of engine as the installed main generators, and should therefore be used for further simulations.

Other sources affecting the fuel consumption variation of each power generator are e.g. operational hours, service intervals, age, and sooting due to low loads among others. All these factors affect the efficiency of the generator set, and thus, give variation in measurements and actual fuel consumption. As operational hours increase, the engine is subject to more wear and tear, especially if the service intervals are infrequent, which can lead to increased specific fuel oil consumption. Engines running on low loads are prone to sooting, primarily due to incomplete combustion, further contributing to higher specific fuel oil consumption. These sources will affect the simulation model’s accuracy. However, the application of the model is to evaluate engine size and configurations to reduce emis-

sions and fuel consumption by using the engines more optimally, between 65-90%, ref. Figure 7. Therefore, the model accuracy on lower loads is satisfactory since an engine optimisation analysis will preferably try to operate engines at higher loads.

A model assumption applied while fitting the SFOC models to the dataset is that the engine characteristics apply after vertically shifting these curves to fit the datasheet data point of the engine. Figure 8 illustrates that, in the case of lower loads, the SFOC<sub>1</sub> model estimates a higher specific fuel consumption when compared to the SFOC<sub>2</sub> model. However, on loads above 35%, the SFOC<sub>2</sub> model estimates greater specific fuel consumption values than the SFOC<sub>1</sub> model. This indicates that SFOC<sub>1</sub> may underestimate fuel consumption on higher loads by assuming ideal test rig conditions, while the SFOC<sub>2</sub> model considers the engine transients and deviation from ideal test rig values, ref. Figure 6.

The motivation for creating the SFOC models was that the supplied information from the engine manufacturers only provided data on the most efficient operation of a new engine. This usually corresponds to loads above 50%, and few or none below 25%. The data analysis performed in this study shows that most of the time the engines run between 8 - 70% load, ref. histogram in Figure 9. The collected data did not have a logging system on fuel consumption. Hence, it was necessary to develop the SFOC models for all engine loads to simulate the fuel consumption of the given operational profile, ref. histogram in Figure 9.

## 4 Conclusions

An SFOC model (SFOC<sub>1</sub>) was developed based on lab measurements for a small engine ( $N_C$ ). SFOC<sub>1</sub> was used to simulate the fuel consumption of Vessel A, and the results were further compared to measured accumulated fuel consumption data. The curve fitting and model assumptions to fit this curve to another engine size showed promising results. The SFOC<sub>1</sub> model simulated an accumulated fuel consumption of 3.9% lower than the measured onboard consumption.

The SFOC<sub>2</sub> model was developed using a regression analysis based on logged fuel consumption data collected from another vessel (Vessel B), and an engine similar to the installed main engines on Vessel A. The results showed that the model simulated an accumulated fuel consumption of 0.9% less than the fuel consumption measured onboard. The regression analysis revealed standard deviations exceeding 10% for loads below 65%. The results show that loads above 65% are preferable regarding specific fuel oil consumption and model accuracy. The data deviation is probably due to gear changes and other sources affecting engine ef-

efficiency, e.g., operational hours, service intervals, age, sooting, etc. These factors would cause the SFOC to increase with operation time. The model's accuracy also heavily depends on the engine load, and the results show that the models are less accurate on lower loads.

Collected data on the engine in Vessel B shows that

the actual consumption is higher than the best-case scenario datasheet value given by the engine manufacturer. This value results from engine performance tests conducted on a test rig on land in a steady-state environment while the engine is new. The  $SFOC_1$  model assumes that the datasheet values represent the fuel consumption, thus not taking transients and other engine

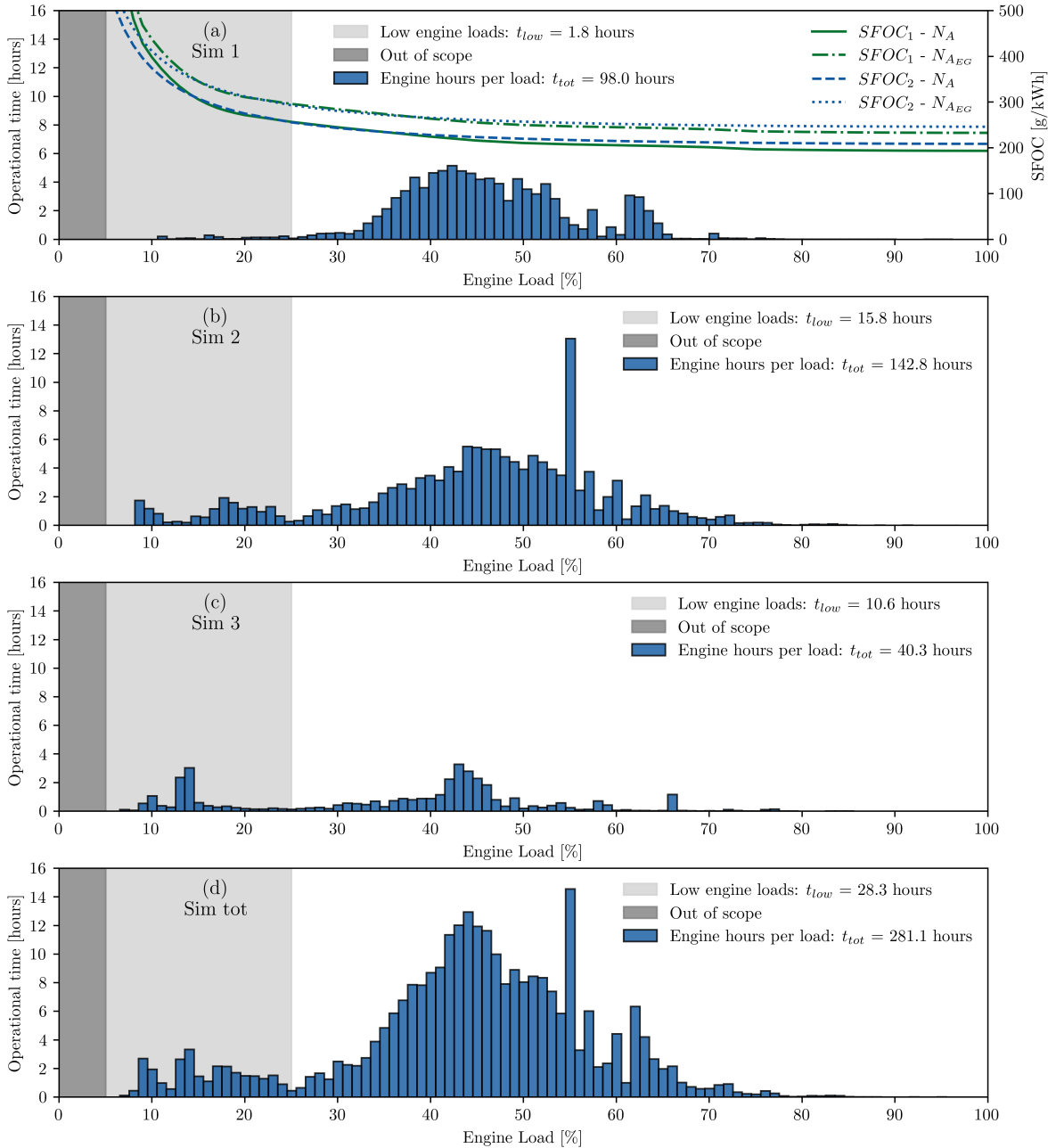


Figure 12: Histograms showing number of operational hours per engine load for (a) simulation period 1, (b) simulation period 2, (c) simulation period 3 and (d) the total simulation period. The two SFOC models  $SFOC_1$  and  $SFOC_2$  are plotted for the main generators  $N_{A_1} - N_{A_4}$  and the emergency generator  $N_{A_{EG}}$  for Case 1 and Case 2 respectively.

efficiency sources into account. The results show that SFOC<sub>2</sub> consequently simulate 2.2-3.3% higher fuel consumption as compared to SFOC<sub>1</sub>. The SFOC<sub>2</sub> model is based on the actual measurement of an engine onboard a ship, thus considering transients and other factors.

Simulation results also revealed that the engine ran 28.3 hours on loads lower than 25% due to redundancy reasons and a too-small port/emergency generator. Hence, the vessel may benefit from optimisation analysis to investigate fuel-saving potential by installing batteries and running the engines on higher loads.

The two SFOC models show promising results for fuel consumption prediction and optimisation purposes. This study concludes that the framework and SFOC models are validated and sufficiently accurate for predicting and optimising fuel consumption and optimising engine configuration and operation. For optimisation, the goal is to operate the engines at loads above 65%.

## 5 Future work

Further work should include a case study evaluating engine configurations and installing a battery package for redundancy and peak shaving. Since the SFOC<sub>2</sub> model used data from an engine of comparable type and size, thus providing a model closer to the vessel’s installed engine, further simulations should use the SFOC<sub>2</sub> model. The framework should be adjusted to include a battery. Simulations could then be run using the optimal power distribution function and be improved to include a battery.

## References

BunkerOil. MGO. n.d. URL <https://www.bunkeroil.no/no/kategori/mgo>. Date accessed: 2023-10-26.

Cluster, B. M. Maritime Industry to cut 50% GHG - Blue Maritime Cluster. 2022. URL <https://www.blumaritimecluster.no/gce/news/news/maritime-industry-to-cut-50-ghg/>.

Dedes, E. K., Hudson, D. A., and Turnock, S. R. Assessing the potential of hybrid energy technology to reduce exhaust emissions from global shipping. *Energy Policy*, 2012. 40:204–218. doi:10.1016/j.enpol.2011.09.046.

DNV. Marine Aquaculture Forecast to 2050 DNV. Technical report, 2021. URL <https://www.dnv.com/Publications/marine-aquaculture-forecast-to-2050-202391>.

Doundoulakis, E. and Papaefthimiou, S. A comparative methodological approach for the calculation of ships air emissions and fuel-energy consumption in two major Greek ports. *Maritime Policy & Management*, 2022. 49(8):1135–1154. doi:10.1080/03088839.2021.1946610.

Fan, A., Yang, J., Yang, L., Wu, D., and Vladimir, N. A review of ship fuel consumption models. *Ocean Engineering*, 2022. 264:112405. doi:10.1016/j.oceaneng.2022.112405.

Ghimire, P., Zadeh, M., Thorstensen, J., and Pedersen, E. Data-Driven Efficiency Modeling and Analysis of All-Electric Ship Powertrain: A Comparison of Power System Architectures. *IEEE Transactions on Transportation Electrification*, 2022. 8(2):1930–1943. doi:10.1109/TTE.2021.3123886.

Henry, M. P., Clarke, D. W., Archer, N., Bowles, J., Leahy, M. J., Liu, R. P., Vignos, J., and Zhou, F. B. A self-validating digital Coriolis mass-flow meter: an overview. *Control Engineering Practice*, 2000. 8(5):487–506. doi:10.1016/S0967-0661(99)00177-X.

IMO, I. Initial IMO GHG Strategy. 2018. URL <https://www.imo.org/en/MediaCentre/HotTopics/Pages/Reducing-greenhouse-gas-emissions-from-ships.aspx>.

Industri, N. SUMMARY: ROADMAP FOR THE AQUACULTURE INDUSTRY. Technical report, 2016. URL [https://www.norskindustri.no/siteassets/dokumenter/rapporter-og-brosjyrer/veikart-for-havbruksnaringen--kortversjon\\_eng.pdf](https://www.norskindustri.no/siteassets/dokumenter/rapporter-og-brosjyrer/veikart-for-havbruksnaringen--kortversjon_eng.pdf).

ISO, J. ISO 15016:2015(en), Ships and marine technology — Guidelines for the assessment of speed and power performance by analysis of speed trial data. 2015. URL <https://www.iso.org/obp/ui/en/#iso:std:61902:en>.

Kim, K.-S. and Roh, M.-I. ISO 15016:2015-Based Method for Estimating the Fuel Oil Consumption of a Ship. *Journal of Marine Science and Engineering*, 2020. 8(10):791. doi:10.3390/jmse8100791.

Law, A. M. How to Build Valid and Credible Simulation Models. In *2022 Winter Simulation Conference (WSC)*. pages 1283–1295, 2022. doi:10.1109/WSC57314.2022.10015411. ISSN: 1558-4305.

Lu, R., Turan, O., Boulougouris, E., Banks, C., and Incecik, A. A semi-empirical ship operational performance prediction model for voyage optimization towards energy efficient ship-

- ping. *Ocean Engineering*, 2015. 110:18–28. doi:10.1016/j.oceaneng.2015.07.042. [a78ecf5ad2344fa5ae4a394412ef8975/en-gb/pdfs/stm202020210013000engpdfs.pdf](https://doi.org/10.1016/j.oceaneng.2015.07.042).
- Mair, G. C., Halwart, M., Derun, Y., and Costa-Pierce, B. A. A decadal outlook for global aquaculture. *Journal of the World Aquaculture Society*, 2023. 54(2):196–205. doi:10.1111/jwas.12977.
- Miljødirektoratet, t. D. f. t. E. Miljøsmål 5.2. 2023. URL <https://miljostatus.miljodirektoratet.no/miljomal/klima/miljomal-5.2>.
- Mylonopoulos, F., Polinder, H., and Coraddu, A. A Comprehensive Review of Modeling and Optimization Methods for Ship Energy Systems. *IEEE Access*, 2023. 11:32697–32707. doi:10.1109/ACCESS.2023.3263719.
- NHO. Green Shipping Challenge. 2022. URL <https://www.nho.no/tema/energi-miljo-og-klima/artikler/green-shipping-challenge/>.
- Nogva. Engine data sheet on 4045TFM50. n.d. URL <http://www.nogva.no/en/products/auxiliary/john-deere/4045tfm50>. Publisher: Nogva Motorfabrikk AS, Date accessed: 2022-02-09.
- Regjeringen, K.-o. M. d. Prop. 1 S (2022–2023) (Proposisjon til Stortinget (forslag til stortingsvedtak)). 2022. URL <https://www.regjeringen.no/no/dokumenter/prop.-1-s-20222023/id2930910/>.
- Regjeringen, N. M. o. C. a. E. Norway’s Climate Action Plan for 2021–2030 Meld. St. 13 (2020–2021) Report to the Storting (white paper). 2021. URL <https://www.regjeringen.no/contentassets/>
- StakeholdersAS and ZeroKyst. Kartlegging av utslipp fra fiskeri og havbruk i Norge. 2022. URL <https://zerokyst.no/wp-content/uploads/2022/08/Rapport-endelig-ZeroKyst-juni-2022.pdf>.
- Sølvtrans. Fleet. 2023. URL <https://www.solvtrans.no/fleet>.
- UN, U. N. The Paris Agreement, UNFCCC. 2015. URL <https://unfccc.int/process-and-meetings/the-paris-agreement/the-paris-agreement>.
- Winther, U., Hognes, E. S., Jafarzadeh, S., and Ziegler, F. Greenhouse gas emissions of Norwegian seafood products in 2017. 2020. page 116. URL [https://www.sintef.no/contentassets/25338e561f1a4270a59ce25bcbc926a2/report-carbon-footprint-norwegian-seafood-products-2017\\_final\\_040620.pdf/](https://www.sintef.no/contentassets/25338e561f1a4270a59ce25bcbc926a2/report-carbon-footprint-norwegian-seafood-products-2017_final_040620.pdf/).
- Æsøy, L., Piehl, H., and Nerheim, A. R. System Simulation-Based Feasibility and Performance Study of Alternative Fuel Concepts for Aquaculture Wellboats. In *Volume 4: Ocean Space Utilization*. American Society of Mechanical Engineers, Hamburg, Germany, page V004T05A006, 2022. doi:10.1115/OMAE2022-81106.
- Æsøy, L., Piehl, H., and Nerheim, A. R. Energy consumption and operational profile of a wellboat—Analysis of a field study. *Ocean Engineering*, 2023. 289:116239. doi:10.1016/j.oceaneng.2023.116239.